# Microstructure and optoelectronic properties of gallium-titanium-zinc oxide thin films deposited by magnetron sputtering*

**CHEN Shou-bu** (陈首部)[1], **LU Zhou** (陆轴)[1], **ZHONG Zhi-you** (钟志有)[1,2], **LONG Hao** (龙浩)[1]**, **GU Jin-hua** (顾锦华)[3], **and LONG Lu** (龙路)[1]

*1. College of Electronic Information Engineering, South-Central University for Nationalities, Wuhan 430074, China*

*2. Hubei Key Laboratory of Intelligent Wireless Communications, South-Central University for Nationalities, Wuhan 430074, China*

*3. Center of Experiment Teaching, South-Central University for Nationalities, Wuhan 430074, China*

(Received 25 January 2016; Revised 21 March 2016)



Gallium-titanium-zinc oxide (GTZO) transparent conducting oxide (TCO) thin films were deposited on glass substrates by radio frequency magnetron sputtering. The dependences of the microstructure and optoelectronic properties of GTZO thin films on Ar gas pressure were observed. The X-ray diffraction (XRD) and scanning electron microscopy (SEM) results show that all the deposited films are polycrystalline with a hexagonal structure and have a preferred orientation along the *c*-axis perpendicular to the substrate. With the increment of Ar gas pressure, the microstructure and optoelectronic properties of GTZO thin films will be changed. When Ar gas pressure is 0.4 Pa, the deposited films possess the best crystal quality and optoelectronic properties.

**Document code:** A **Article ID:** 1673-1905(2016)04-0280-5

**DOI** 10.1007/s11801-016-6025-2

ZnO semiconductor thin films offer a wide range of applications in optoelectronic devices, such as solar photovoltaic cells[1-3], flat panel displays[4], light emitting diodes[5,6], chemical sensors[7,8] and resistive switching[9]. Transparent conductive electrode is a necessary component of solar photovoltaic cells. Usually, it consists of a transparent conducting oxide (TCO) thin film and a glass substrate. The most important commercial material for TCOs nowadays is indium-tin oxide (ITO), owing to its unique characteristics of high visible transmittance, low resistivity, high infrared reflectance and absorbance in the microwave region. However, ITO is likely to become unavailable because of the limitation of indium resources and toxicity in the atmosphere. In view of the depletion of ITO, the doped ZnO will be emerging as an alternative transparent electrode. Recently, much attention has been paid to the codoping process in which two elements are doped into ZnO simultaneously, because the codoped ZnO thin films are expected to show some improvements in optical and electrical performance of TCOs. Suzuki et al[10] prepared the vanadium-aluminum codoped ZnO (VAZO) thin films by direct-current magnetron sputtering to enhance the corrosion-resistance of the TCO films. Kirbey et al[11] deposited the aluminum-indium codoped ZnO (AIZO) thin films using off-axis reactive radio frequency sputtering and obtained improved electrical properties with no degradation in optical transmittance. Suresh et al[12] prepared the gallium-indium codoped ZnO (GIZO) thin films by pulsed laser deposition and achieved improved surface morphology with enhanced optoelectronic properties. Up to now, the aluminum- gallium[13], magnesium-gallium[14], aluminum-titanium[15], boron-gallium[16] and magnesium-aluminum[17] codoping cases have also been reported. However, there have been few reports on gallium-titanium codoped ZnO (GTZO) thin films.

In this paper, the GTZO semiconductor thin films were deposited on glass substrates by magnetron sputtering technique. The influence of Ar gas pressure on the grain-growth orientation, microstructure, morphology and optoelectronic properties of the thin films was investigated by X-ray diffraction (XRD), scanning electron microscopy (SEM), ultraviolet-visible spectrophotometer and four-probe meter.

The GTZO thin films were grown on the cleaned glass substrates by using 13.56 MHz radio frequency magnetron sputtering. A sintered GTZO ceramic sputter target (1.5% (weight percentage, the same below) $Ga_2O_3$: 1.5% $TiO_2$: 97% ZnO, 4N purity) was employed as source material. The sputtering chamber was evacuated to a base pressure below $5.5\times10^{-4}$ Pa before Ar gas. After

* This work has been supported by the National Natural Science Foundation of China (No.11504436), the Natural Science Foundation of Hubei Province (No.2015CFB364), and the Fundamental Research Funds for the Central Universities (Nos.CZW14019 and CZW15045).

** E-mail: longscun@126.com

vacuum pumping, the sputtering Ar gas with a purity of 99.999% was introduced into the chamber and controlled by the standard mass flow controllers. Before the GTZO thin films deposition, pre-sputtering was conducted for about 10 min to attain stability and to remove impurities. The deposition parameters for preparing GTZO thin films are as follows: the substrate-target distance was 7.0 cm, the substrate temperature was 340 °C, the sputtering power was 210 W, and the sputtering time was 25 min. In order to investigate the influence of Ar gas pressure on properties of the deposited films, the Ar gas pressure ($P_{Ar}$) was varied from 0.3 Pa to 0.6 Pa. The thickness of the samples was measured by a surface profiler (Alpha-step 500). The surface morphology was observed by an SEM (JSM-6700F). The crystallographic and phase structures were characterized by XRD. A D8-Advance diffractometer with Cu K$\alpha$ source ($\lambda$=0.154 06 nm) and Ni filter was used for the XRD measurement. The power of XRD was 1 200 W and the scan was preformed from 20° to 80° at a speed of 1.872°/min, with a step size of 0.016 4°. The crystallite phase was determined with the data of joint committee on powder diffraction standards (JCPDS). The optical transmission ($T$) and reflection ($R$) spectra at normal incidence were measured with a double-beam UV-visible spectrophotometer (TU-1901), and the electrical properties were evaluated using a four-point probe measurement system (RH-2035). All measurements were carried out in air ambient at room temperature.

Fig.1 shows the XRD patterns of the GTZO samples deposited on glass substrates at different $P_{Ar}$. These XRD peaks are assigned to ZnO according to the JCPDS data file No.36-1451 (ZnO). As can be seen, all the samples exhibit a dominant (002) peak with slight (004) and (100) peaks in the displayed $2\theta$ region, indicating that the GTZO thin films have hexagonal wurtzite structure with high *c*-axis orientation. Neither metallic Ga or Ti characteristic peaks nor $Ga_2O_3$ or $TiO_2$ peaks were observed from the XRD patterns, which implies that the dopants have not destroyed the ZnO structure and act as typical dopants. From Fig.1, the intensity of (002) peak ($I_{(002)}$) is much stronger than that of the others. Corresponding to the $P_{Ar}$ of 0.3 Pa, 0.4 Pa, 0.5 Pa and 0.6 Pa, the $I_{(002)}$ values are observed to be $1.48\times10^6$ cycles per second (cps), $1.65\times10^6$ cps, $5.76\times10^5$ cps and $4.17\times10^5$ cps, respectively. Clearly, the $I_{(002)}$ increases firstly and then decreases with the increase of $P_{Ar}$.

The texture coefficient $TC_{(hkl)}$ of the deposited thin films was calculated from the following equation[17]:

$$TC_{(hkl)} = \frac{I_{(hkl)}/I_{0(hkl)}}{\frac{1}{n}\sum_n \left(I_{(hkl)}/I_{0(hkl)}\right)}, \quad (1)$$

where the subscripts *h*, *k* and *l* are Miller indices, $I_{(hkl)}$ is the measured intensity of a plane (*hkl*), $I_{0(hkl)}$ is the standard intensity of the plane (*hkl*) taken from the JCPDS data file, and *n* is the reflection number of diffraction peaks considered. It is clear from Eq.(1) that the deviation of texture coefficient from unity implies the thin film growth in preferred orientation. The calculated texture coefficients $TC_{(hkl)}$ are plotted in the inset of Fig.1. As can be seen, the values of $TC_{(100)}$, $TC_{(002)}$ and $TC_{(004)}$ are 0.002 35—0.004 96, 2.921—2.961 and 0.034 3—0.042 3, respectively. Obviously, the highest $TC_{(hkl)}$ values are in (002) plane for all the deposited films, suggesting that all the deposited films have *c*-axis preferred orientation. As shown in the inset of Fig.1, with increasing the $P_{Ar}$ from 0.3 Pa to 0.4 Pa, the $TC_{(002)}$ increases, indicating that the crystal quality of the GTZO thin films becomes better. However, with further increasing the $P_{Ar}$ from 0.4 Pa to 0.6 Pa, the $TC_{(002)}$ gradually decreases and the crystal quality deteriorates. The maximal $TC_{(002)}$ of 2.961 is obtained for the sample deposited at $P_{Ar}$=0.4 Pa. The results indicate that the GTZO thin films deposited at $P_{Ar}$=0.4 Pa possess the best crystallite quality.

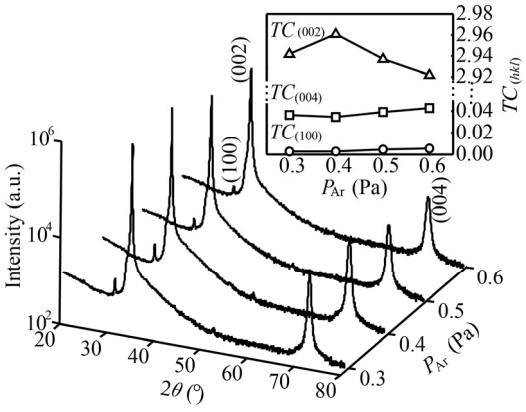


**Fig.1 XRD patterns of GTZO samples deposited at different $P_{Ar}$**

Fig.2 displays a typical SEM image of the sample deposited at $P_{Ar}$=0.4 Pa. It depicts that the surface of GTZO film is smooth and dense, and the grain size is uniformly distributed with an average size of about 90 nm. The thin film consists of some columnar structured and *c*-axis oriented grains, which is consistent with the result of XRD.

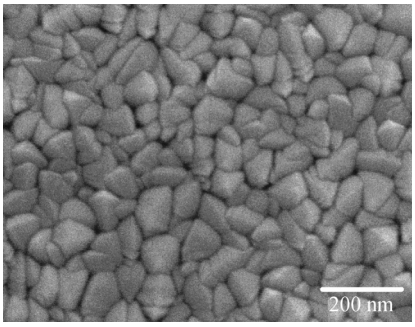


**Fig.2 SEM image of the GTZO sample deposited at $P_{Ar}$=0.4 Pa**

The crystallite size of the deposited films was calculated from the diffraction peaks of (002) plane using Debye-Scherrer's (DS) formula[18,19]:

$$D = \frac{k\lambda}{B\cos\theta_B}, \tag{2}$$

where $D$, $k$, $\lambda$, $\theta_B$ and $B$ are the mean crystallite size, the Scherrer factor ($k$≈0.89), the X-ray wavelength ($\lambda$=0.154 06 nm), the Bragg diffraction angle, and the full-width at half-maximum (*FWHM*), respectively. The dislocation density $\delta$ and the strain $\varepsilon$ can be estimated from the following formulae[8,20]:

$$\delta = D^{-2}, \tag{3}$$

$$\varepsilon = \frac{c - c_0}{c_0}, \tag{4}$$

where $c$ and $c_0$ are the lattice constants of the deposited films and pure ZnO, respectively. The lattice constants of the deposited films were calculated from XRD data using the following equation[20]:

$$\frac{1}{(0.5\lambda/\sin\theta)^2} = \frac{4}{3}\left(\frac{h^2 + hk + k^2}{a^2}\right) + \frac{l^2}{c^2}, \tag{5}$$

where $a$ and $c$ are the lattice constants. The stress $\sigma$ in the plane of the thin film can be evaluated using the biaxial strain model[14]:

$$\sigma \approx -233\times10^9\varepsilon \quad \text{(Pa)}. \tag{6}$$

The values of $D$, $\delta$, $\varepsilon$ and $\sigma$ of all the deposited films are presented in Fig.3 and Fig.4, respectively. For the GTZO samples prepared at $P_{Ar}$ of 0.3 Pa, 0.4 Pa, 0.5 Pa and 0.6 Pa, the $D$ values are found to be 73.9 nm, 87.5 nm, 45.0 nm and 37.9 nm, respectively, as shown in Fig.3. The crystallite size $D$ increases first and subsequently decreases with the increment of $P_{Ar}$. The sample deposited at 0.4 Pa possesses the largest crystallite size of 87.5 nm. The increase in crystallite size may be due to the coalescence of small crystals. From Fig.3 and Fig.4, the $\delta$ and $\varepsilon$ values are obtained to be in the ranges of $1.31\times10^{14}$—$6.96\times10^{14}$ line·m$^{-2}$ and $8.25\times10^{-4}$—$1.36\times10^{-3}$, respectively. And the tendency in the change of $\delta$ and $\varepsilon$ is observed to be opposite to that of $D$. Clearly, the sample prepared at 0.4 Pa exhibits the minimum $\delta$ and $\varepsilon$. The decrease in $\delta$ and $\varepsilon$ can be attributed to the improvement of crystallinity and the increase of crystallite size. From Fig.4, it can be seen that all the samples have a negative stress, which indicates a compressive stress in the deposited films. The values of $\sigma$ are $2.81\times10^8$ Pa, $1.90\times10^8$ Pa, $2.62\times10^8$ Pa and $3.24\times10^8$ Pa for the films deposited at $P_{Ar}$ of 0.3 Pa, 0.4 Pa, 0.5 Pa and 0.6 Pa, respectively. The $\sigma$ value of the thin films is observed to decrease firstly and then increase with the increase of $P_{Ar}$. The results suggest that the crystallite size, dislocation density, strain and stress of the deposited films are subjected to the $P_{Ar}$.

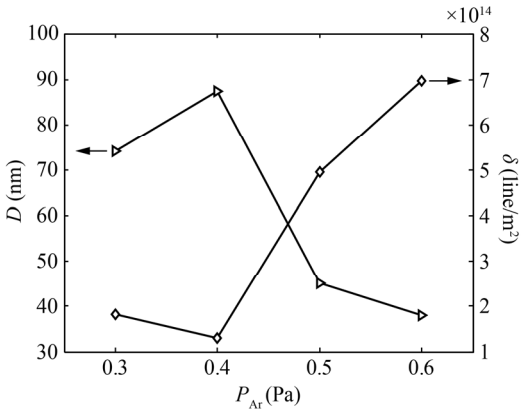


**Fig.3 The $D$ and $\delta$ values of GTZO samples deposited at different $P_{Ar}$**

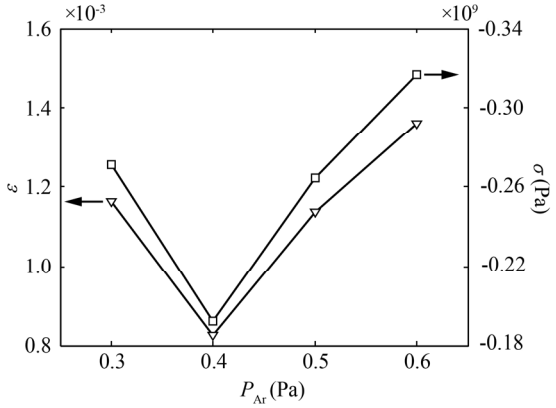


**Fig.4 The $\varepsilon$ and $\sigma$ values of GTZO samples deposited at different $P_{Ar}$**

The transmission ($T$) and reflection ($R$) spectra at normal incidence for GTZO samples deposited at different $P_{Ar}$ are presented in Fig.5. All the transmission

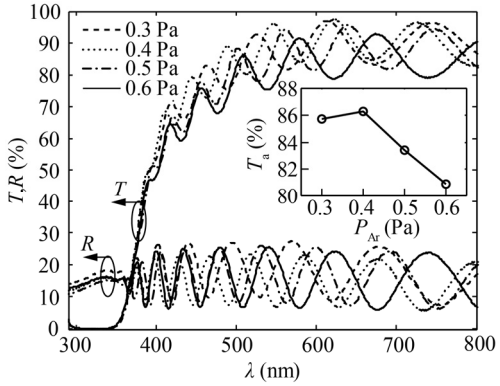


**Fig.5 The spectra of $T$ and $R$ for GTZO samples deposited at different $P_{Ar}$**

spectra show interference pattern with sharp fall of transmittance at the band edge, which is an indication of good crystallinity. As shown in the inset of Fig.5(a), the average transmittance in the visible range ($T_a$) increases

slightly with the $P_{Ar}$ up to 0.4 Pa, and then significantly decreases when the $P_{Ar}$ is over 0.4 Pa. The highest $T_a$ value of 86.31% can be achieved at $P_{Ar}$=0.4 Pa. This enhancement in the optical transmittance is closely related to the improvement of crystallinity and the increase of crystallite size of the thin films.

Fig.6 shows the Tauc plots of $(\alpha h\nu)^2$ as a function of photon energy $h\nu$ for the GTZO samples deposited at different $P_{Ar}$. As a direct band gap semiconductor, the optical band gap $E_g^d$ can be determined by the following equation[21,22]:

$$(\alpha h\nu)^2 = A(h\nu - E_g^d), \tag{7}$$

where $A$ is a constant dependent on the electron-hole mobility, and $\alpha$ is the absorption coefficient, as a function of the photon energy $h\nu$. The $\alpha$ values were calculated from the transmission and reflection spectra using the following formula[21]:

$$\alpha = \frac{1}{d}\ln\left(\frac{(1-R)^2}{T}\right), \tag{8}$$

where $d$ is the film thickness, and $T$ and $R$ are the transmittance and reflectance, respectively. The values of $E_g^d$ are determined by extrapolating the linear portion of the curves to $(\alpha h\nu)^2$=0. The band gaps of GTZO samples were found to be ranging from 3.456 eV to 3.481 eV, larger than that of undoped ZnO (~3.270 eV). The widening of optical band gap may be attributed to Moss-Burstein shift effect[23,24]. This effect is due to the conduction band filling in highly degenerate semiconductor makes the Fermi level exceed the conduction band minimum.

Fig.7 shows the electrical resistivity $\rho$ of the GTZO samples deposited at different $P_{Ar}$. As the $P_{Ar}$ increases from 0.3 Pa to 0.6 Pa, the $\rho$ drops initially and subsequently rises. The lowest $\rho$ value of $7.23\times10^{-4}$ Ω·cm is obtained for the GTZO sample deposited at $P_{Ar}$=0.4 Pa. The reduction in the electrical resistivity can be attributed to the improvement of crystallinity and the increase of crystallite size[25].

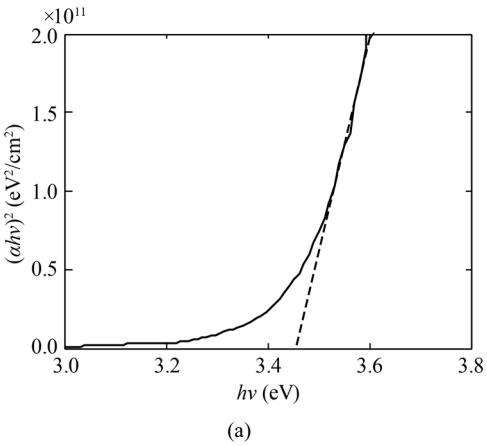


(a)

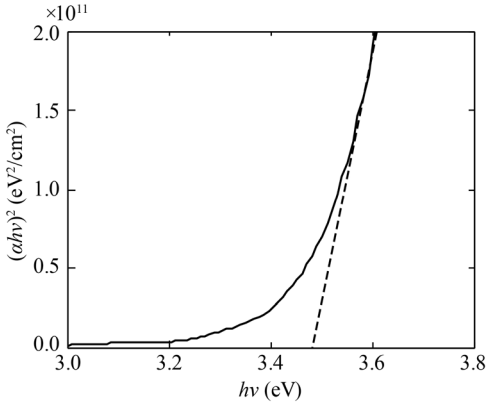


(b)

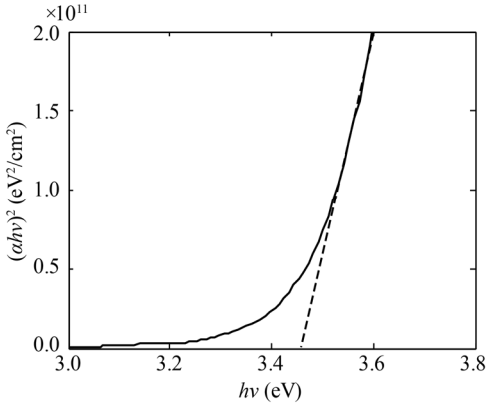


(c)

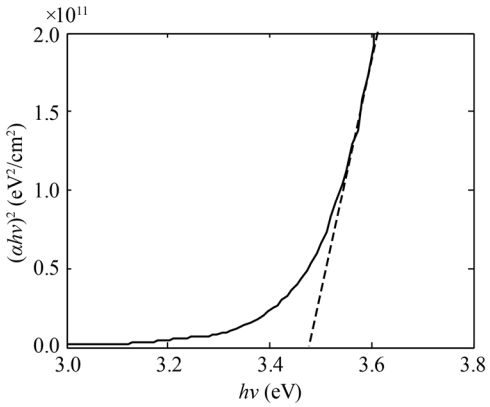


(d)

**Fig.6 Tauc plots of $(\alpha h\nu)^2$ versus $h\nu$ for GTZO samples deposited at different $P_{Ar}$**

In order to evaluate the quality of the transparent conductors, the figure of merit ($F_{TC}$) is given by the formula[22]:

$$F_{TC} = \frac{T_a}{\rho}, \tag{9}$$

where $T_a$ is the average transmittance in the visible range and $\rho$ is the electrical resistivity. Fig.7 displays the variation of $F_{TC}$ with $P_{Ar}$ for the deposited GTZO samples. As the $P_{Ar}$ increases, the $F_{TC}$ first increases then decreases and reaches its maximum value of $1.19\times10^3$ $\Omega^{-1}\cdot cm^{-1}$ at $P_{Ar}$=0.4 Pa.

The increase in $F_{TC}$ with $P_{Ar}$ is due to the decrease in electrical resistivity and the increase in optical transmittance. It is known that the higher the $F_{TC}$, the better quality of the TCO thin film. Thus, in this study, it can be concluded that the optimum Ar gas pressure is 0.4 Pa, where the $F_{TC}$ is the highest.

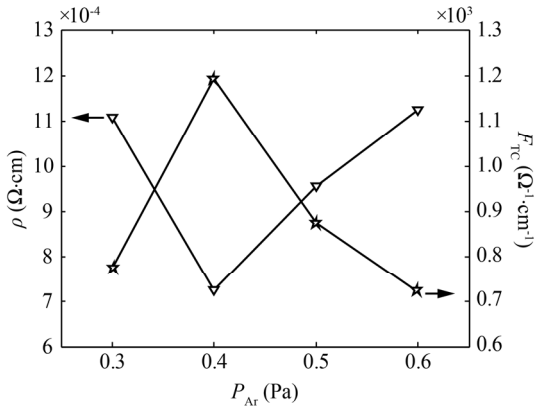


**Fig.7 The $T_a$ and $\rho$ values of GTZO samples deposited at different $P_{Ar}$**

In conclusion, transparent conducting GTZO thin films were deposited by radio frequency magnetron sputtering method. The Ar gas pressure dependences of the grain-growth orientation, structural, optical and electrical properties for the deposited films were investigated by XRD, SEM, four-point probe and spectrophotometer. It is found that the GTZO thin films are polycrystalline and have preferred orientation along (002) direction. The crystalline quality, microstructure and optoelectonic properties of the deposited films are closely related to the Ar gas pressure. As the Ar gas pressure increases, the texture coefficient of (002) plane, crystallite size, average visible transmittance and figure of merit are observed to increase initially and subsequently decrease, whereas the dislocation density, strain, compressive stress and electrical resistivity decrease firstly and then increase. The thin films deposited at the Ar gas pressure of 0.4 Pa exhibit the best crystal quality and optoelectronic properties, with the largest crystallite size of 87.5 nm, the highest average visible transmittance of 86.31%, the lowest resistivity of $7.23\times10^{-4}$ Ω·cm and the maximum figure of merit of $1.19\times10^{3}$ $\Omega^{-1}\cdot cm^{-1}$. In addition, the optical band gaps of the thin films were calculated by means of the Tauc plots. The results show that the band gaps are in the range of 3.456—3.481 eV, larger than that of undoped ZnO due to Burstein-Moss shift.

## References

[1] Song Y S, Seong N J, Choi K J and Ryu S O, Thin Solid Films **546**, 271 (2013).

[2] Zhang Qiang, Qin Wen-jing, Cao Huan-qi, Yang Li-ying, Zhang Feng-ling and Yin Shou-gen, Optoelectron. Lett. **10**, 0253 (2014).

[3] Zhong Z, Lu Z, Long L and Kang H, J. South-Cent. Univ. Nationalities (Nat. Sci. Ed.) **35**, 58 (2016). (in Chinese)

[4] Yamamoto N, Makino H, Osone S, Ujihara A, Ito T, Hokari H, Maruyama T and Yamamoto T, Thin Solid Films **520**, 4131 (2012).

[5] Wang H, Long H, Chen Z, Mo X, Li S, Zhong Z and Fang G, Electron. Mater. Lett. **11**, 664 (2015).

[6] Chen S and Wei S, J. South-Cent. Univ. Nationalities (Nat. Sci. Ed.) **34**, 72 (2015). (in Chinese)

[7] Hjiri M, Mir L E, Leonardi S G, Pistone A, Mavilia L and Neri G, Sensor. Actuat. B **196**, 413 (2014).

[8] Barhoumi A, Leroy G, Duponchel B, Gest J, Yang L, Waldhoff N and Guermazi S, Superlattice Microst. **82**, 483 (2015).

[9] Santos D A A, Zeng H and Macêdo M A, Mater. Res. Bull. **66**, 147 (2015).

[10] Suzuki S, Miyata T, Ishii M and Minami T, Thin Solid Films **434**, 14 (2003).

[11] Kirbey S D and Van Dover R B, Thin Solid Films **517**, 1958 (2009).

[12] Suresh A, Wellenius P, Dhawan A and Muth J, Appl. Phys. Lett. **90**, 123512 (2007).

[13] Ebrahimifard R, Golobostanfard M R and Abdizadeh H, Appl. Surf. Sci. **290**, 252 (2014).

[14] Liu J, Chen X, Fang J, Zhao Y and Zhang X, Solar Energy Mater. Solar Cells **138**, 41 (2015).

[15] Davoodi A, Tajally M, Mirzaee O and Eshaghi A, J. Alloy. Compd. **657**, 296 (2016).

[16] Zhang L, Huang J, Yang J, Tang K, Ren B, Hu Y, Wang L and Wang L, Mater. Sci. Semicond. Process. **42**, 277 (2016).

[17] Fang D, Lin K, Xue T, Cui C, Chen X, Yao P and Li H, J. Alloy. Compd. **589**, 346 (2014).

[18] Huang Z, Long J, Wu L and Liu X, J. South-Cent. Univ. Nationalities (Nat. Sci. Ed.) **34**, 10 (2015). (in Chinese)

[19] Fu Chang-feng, Chen Xi-ming, Li Lan, Han Lian-fu and Wu Xiao-guo, Optoelectron. Lett. **6**, 0037 (2010).

[20] Zhong Z, Lan C, Long L and Lu Z, J. South-Cent. Univ. Nationalities (Nat. Sci. Ed.) **34**, 66 (2015). (in Chinese)

[21] Pankove J I, Optical Processes in Semiconductors, New York: Dover Publications, 1975.

[22] Gu J, Long L, Lu Z, Zhang T and Zhong Z, J. South-Cent. Univ. Nationalities (Nat. Sci. Ed.) **34**, 68 (2015). (in Chinese)

[23] Liu Jie-ming, Chen Xin-liang, Tian Cong-sheng, Liang Jun-hui, Zhang De-Kun, Zhao Ying and Zhang Xiao-dan, Journal of Optoelectronics·Laser **25**, 2214 (2014). (in Chinese)

[24] Zi Xing-fa, Ye Qing, Liu Rui-ming and He Yong-tai, Journal of Optoelectronics·Laser **26**, 883 (2015). (in Chinese)

[25] Zhu H, Hüpkes J, Bunte E, Gerber A and Huang S M, Thin Solid Films **518**, 4997 (2010).